Supporting Information

An uncommon 3D 3,3,4,8-c Cd(II) metal-organic framework for highly efficient luminescent sensing and organic dye adsorption: experimental and theoretical insight

Lu Lu[a*], Jian Wu[b], Jun Wang[a], Jian-Qiang Liu[c], Bao-Hong Li[c*], Amita Singh[d], Abhinav Kumar[d*] and Stuart R. Batten[e]

Sensing Method

The photoluminescence sensing were performed as follows: the photoluminescence properties of **1** were investigated in N,N-dimethylformamide (DMF)/H_2O emulsions at room temperature using a RF-5301PC spectrofluorophotometer. The **1**@DMF/H_2O elusions were prepared by adding 5 mg of **1** powder into 3.00 mL of DMF and then ultrasonic agitation the mixture for 30 min before testing.

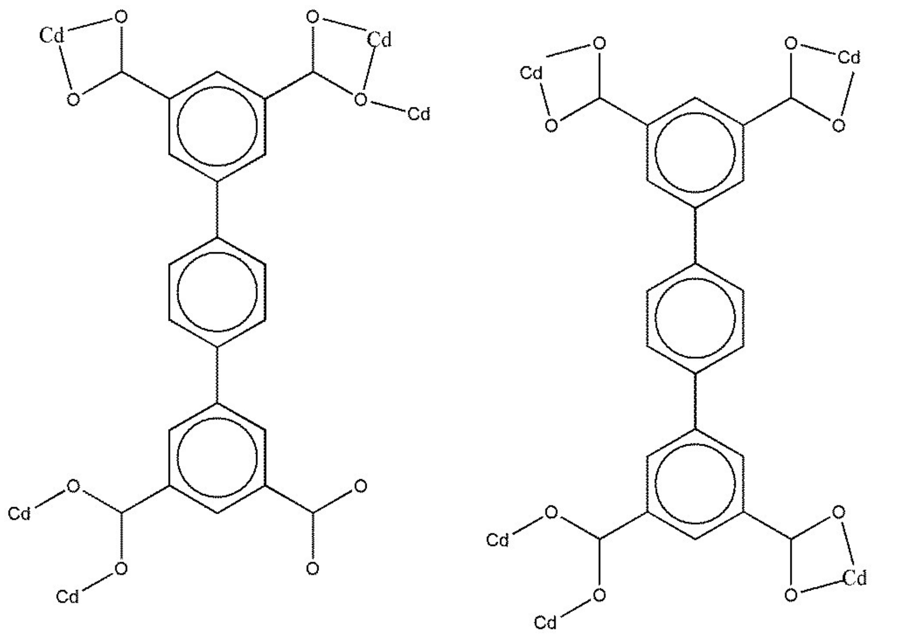

(a) (b)

Scheme S1 view of the different coordination modes of H_4L ligand in this work.

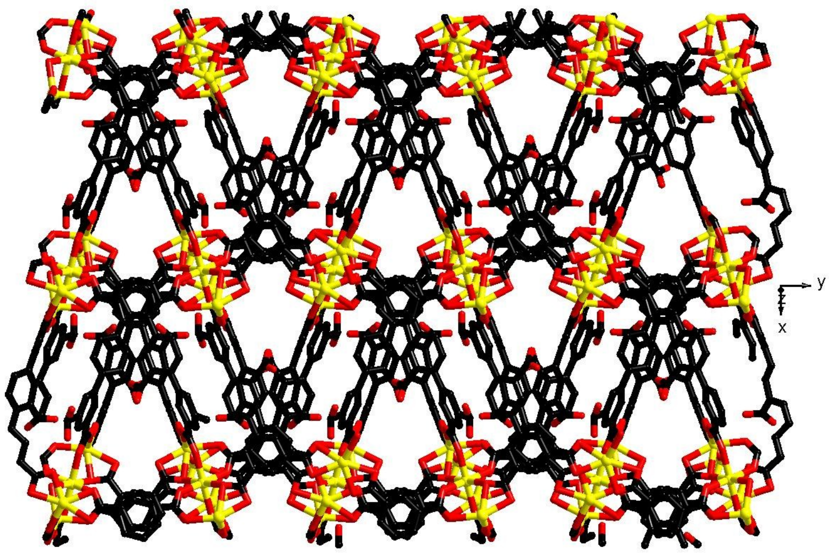

Fig.S1 view of the 3D network.

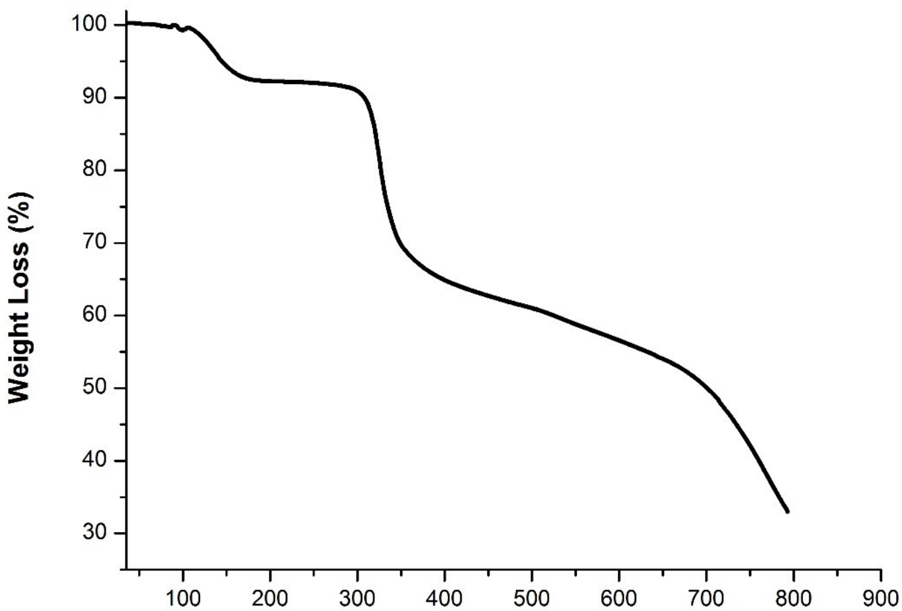

Fig. S2 view of TGA in **1**.

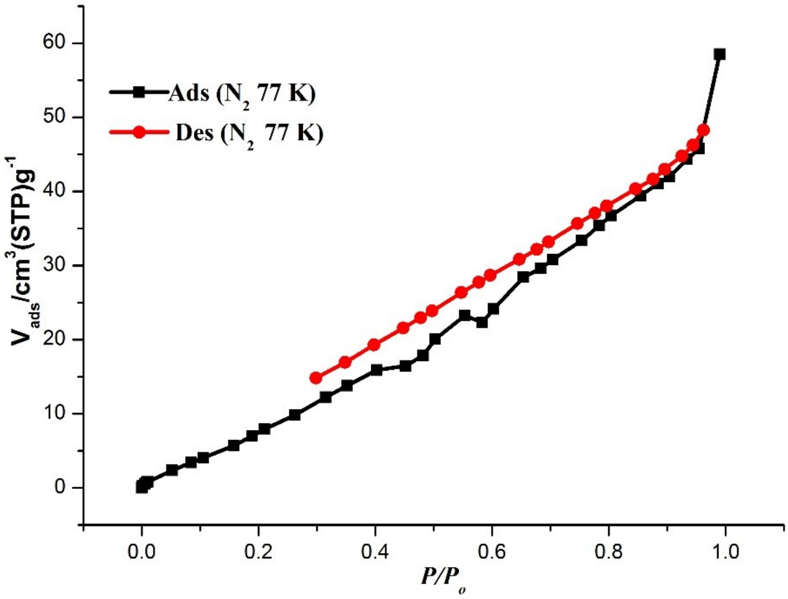

Fig. S3 view of the N_2 adsorption isotherms at 77 K.

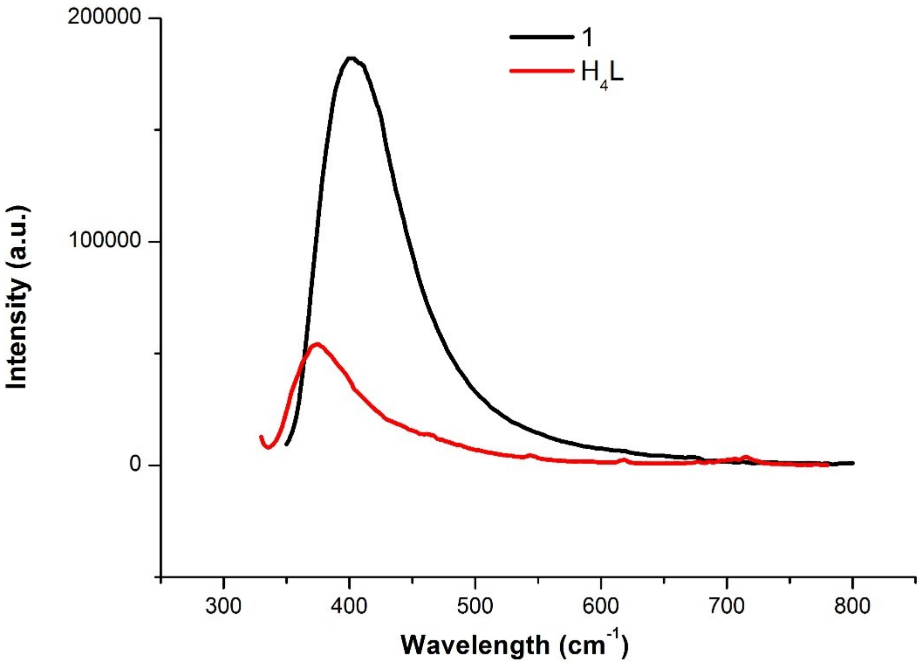

Fig. S4 view of the PL for solid state of **1** and H_4L at room temperature.

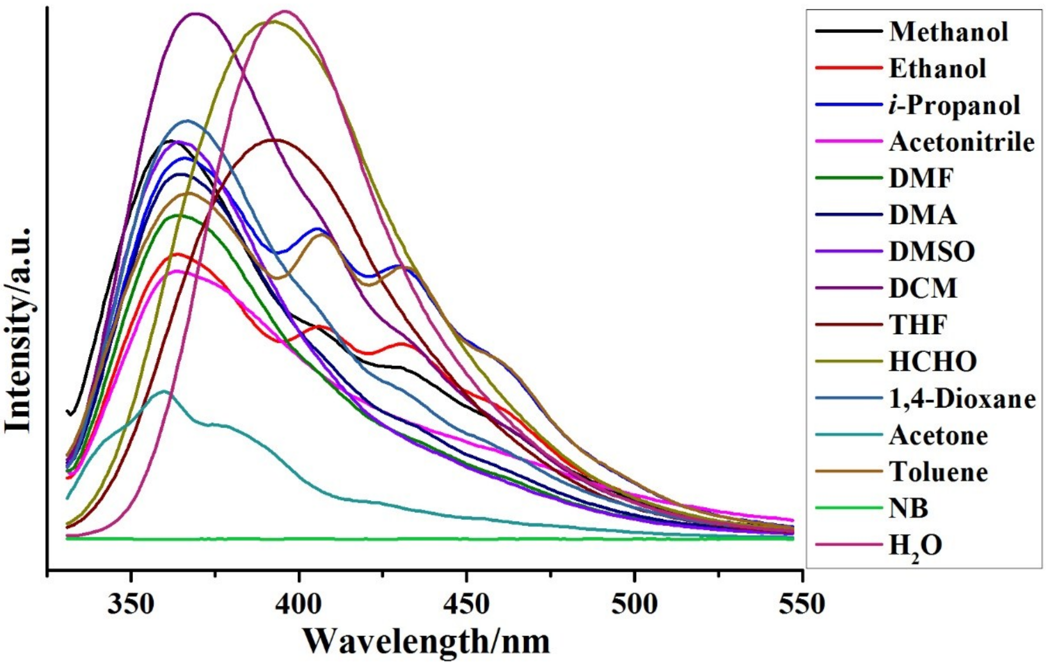

Fig. S5 Emission spectra of **1** at different solvents.

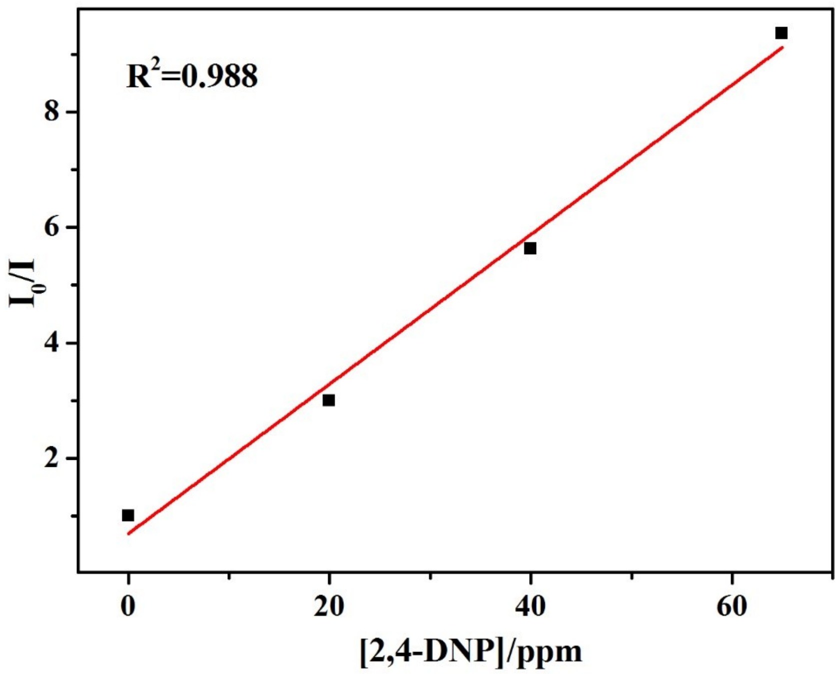

Fig. S6 Stern–Volmer plot for the fluorescence quenching of **1** upon the addition of 2,4-DNP.

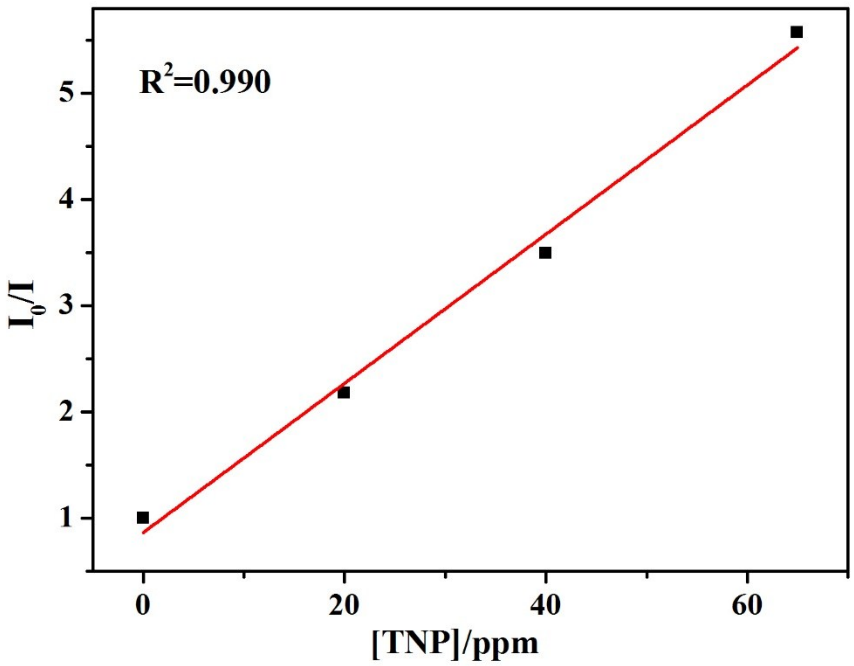

Fig. S7 Stern–Volmer plot for the fluorescence quenching of **1** upon the addition of TNP.

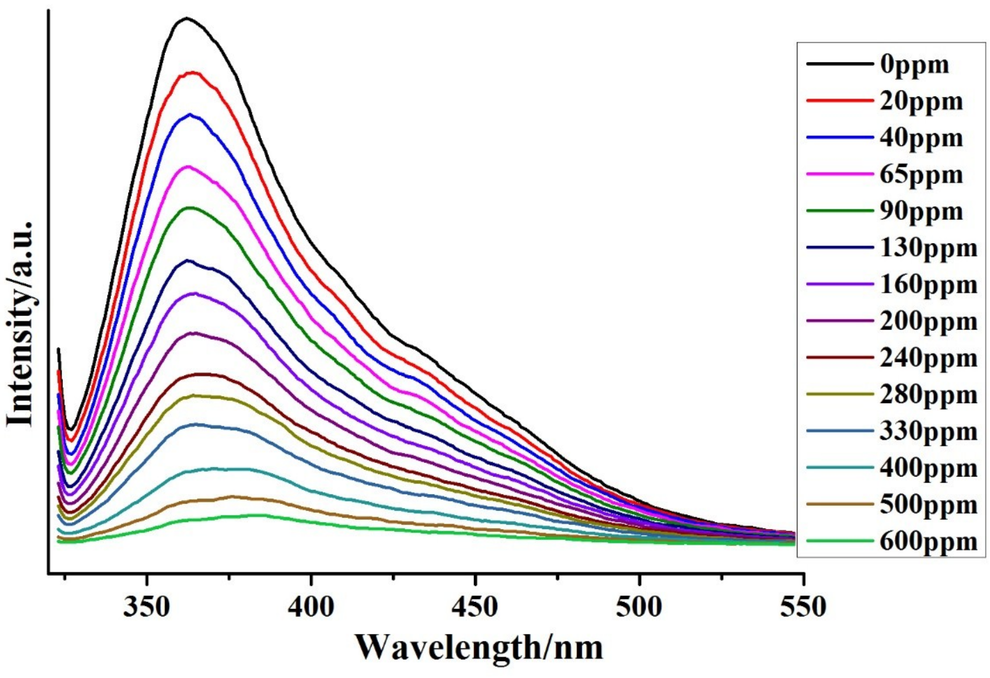

Fig. S8 Luminescent quenching of **1** dispersed in ethanol by the gradual addition of 1 mM solution of 1,3-DNB in DMF.

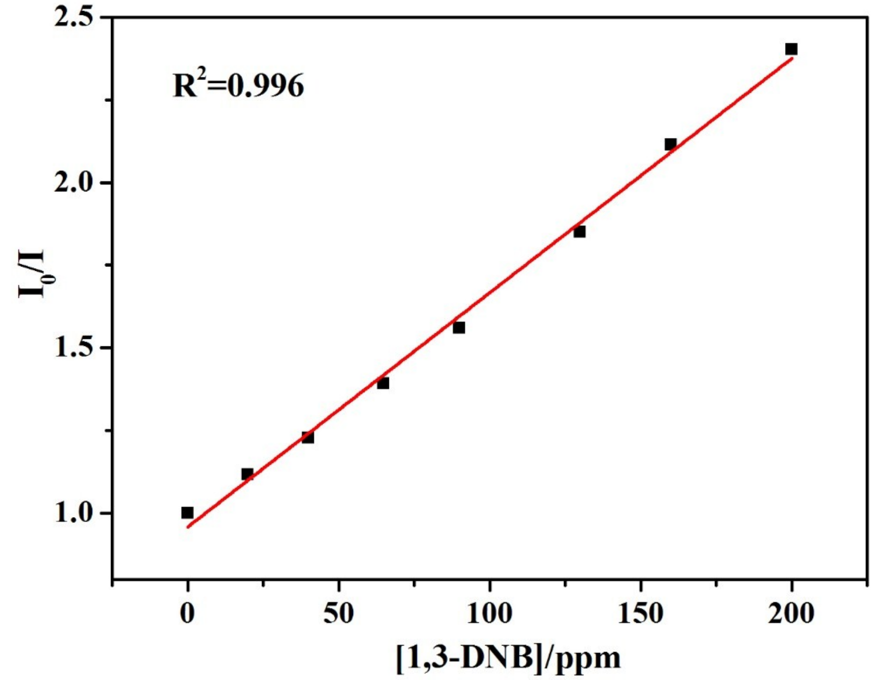

Fig. S9 Stern–Volmer plot for the fluorescence quenching of **1** upon the addition of 1,3-DNB.

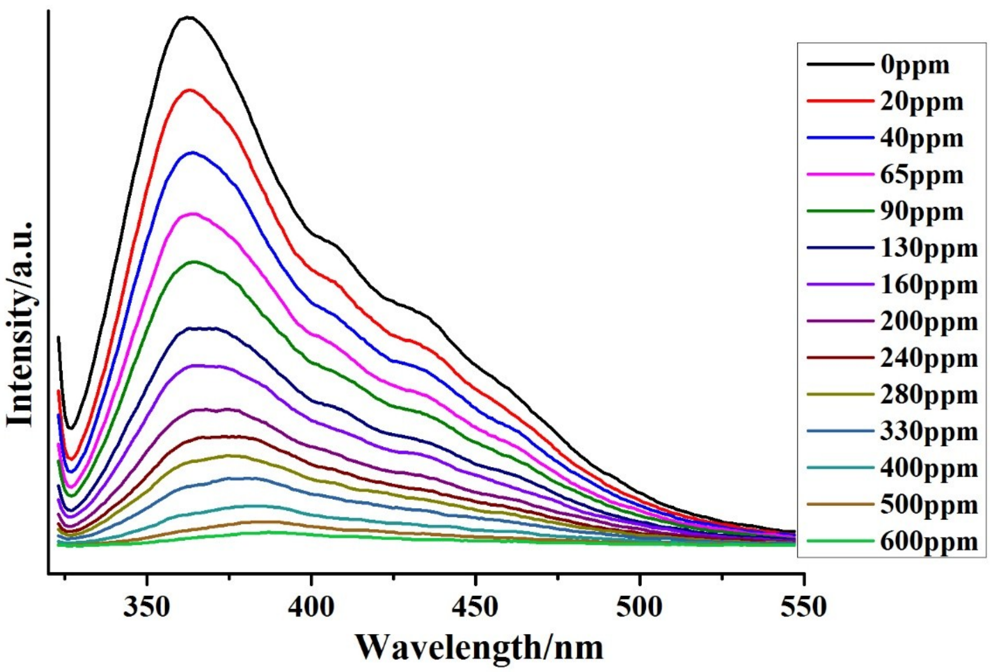

Fig. S10 Luminescent quenching of **1** dispersed in ethanol by the gradual addition of 1 mM solution of 2,4-DNT in DMF.

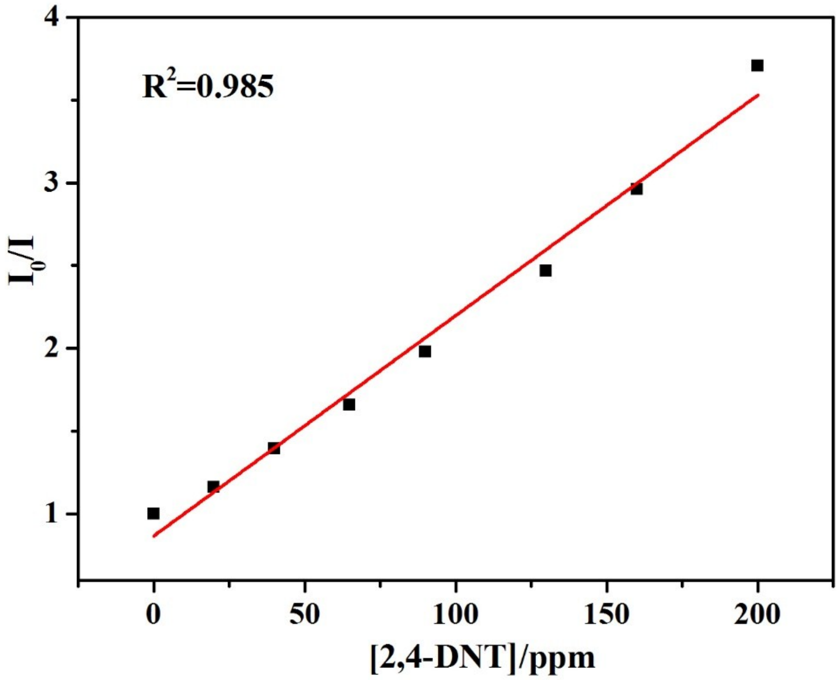

Fig. S11 Stern–Volmer plot for the fluorescence quenching of **1** upon the addition of 2,4-DNT.

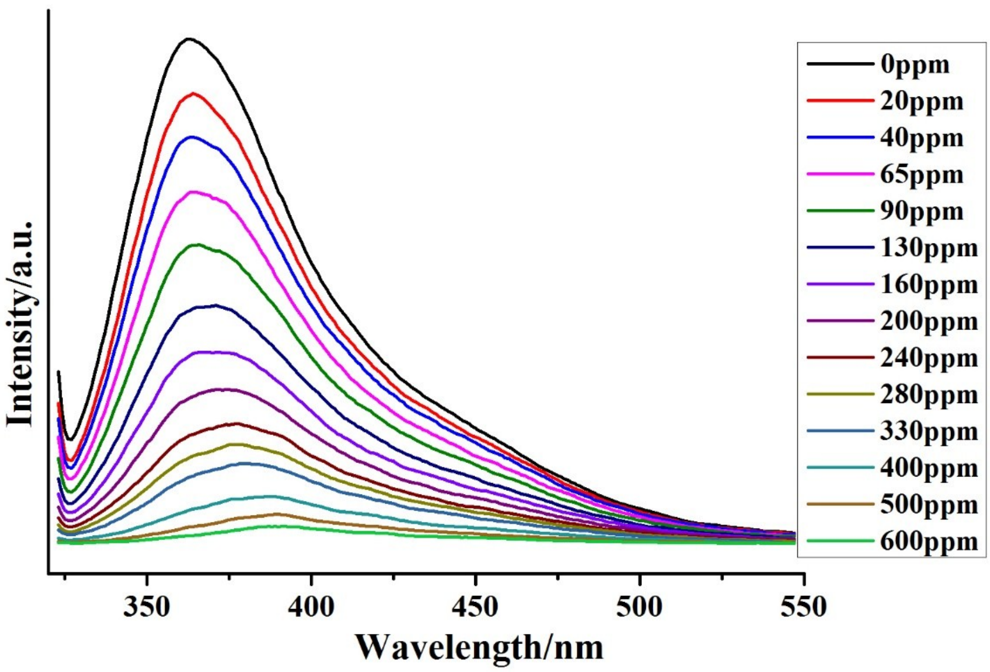

Fig. S12 Luminescent quenching of **1** dispersed in ethanol by the gradual addition of 1 mM solution of 2,6-DNT in DMF.

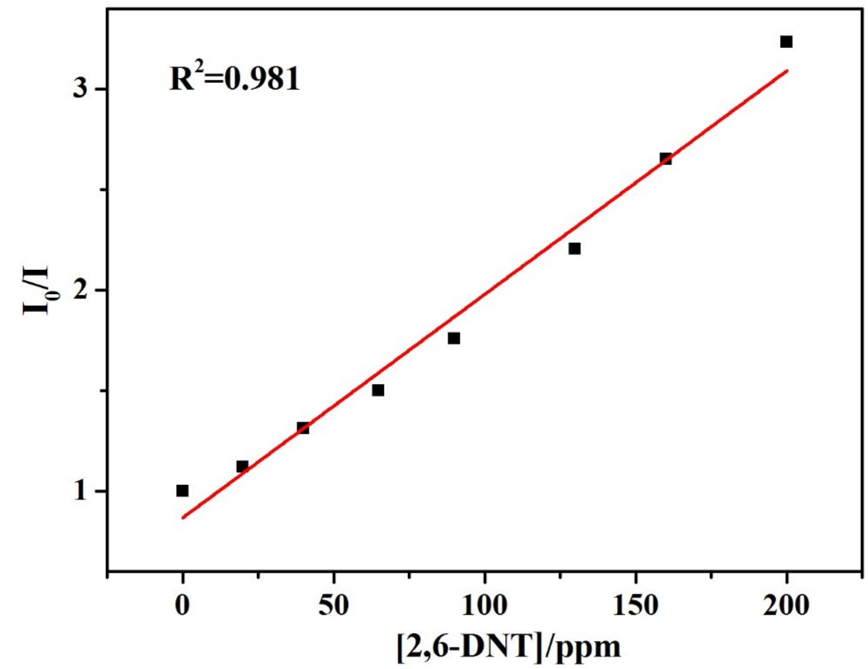

Fig. S13 Stern–Volmer plot for the fluorescence quenching of **1** upon the addition of 2,6-DNT.

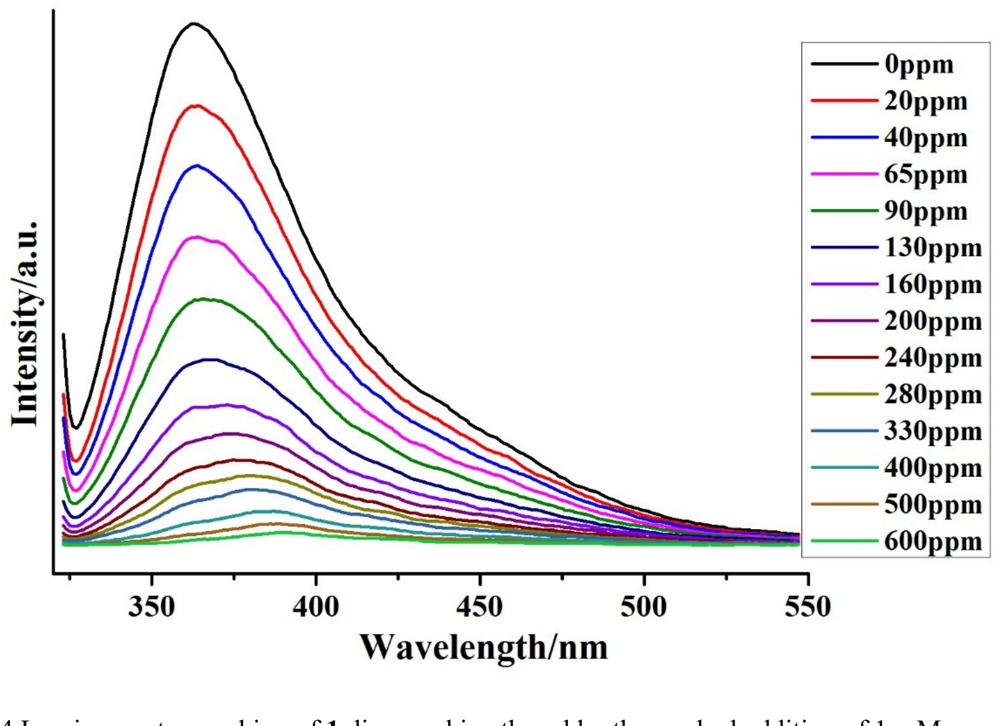

Fig. S14 Luminescent quenching of **1** dispersed in ethanol by the gradual addition of 1 mM solution of 2-NT in DMF.

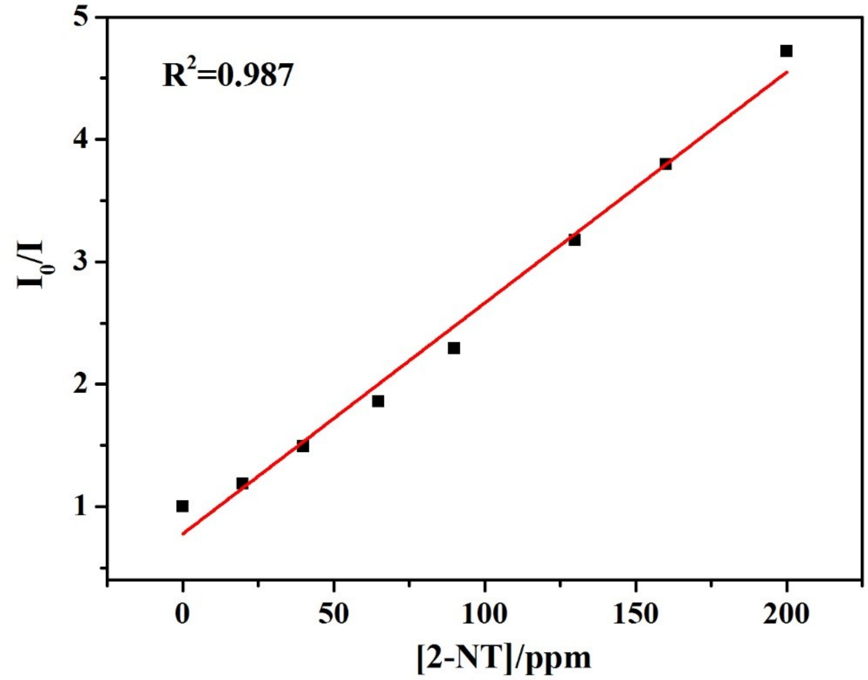

Fig. S15 Stern–Volmer plot for the fluorescence quenching of **1** upon the addition of 2-NT.

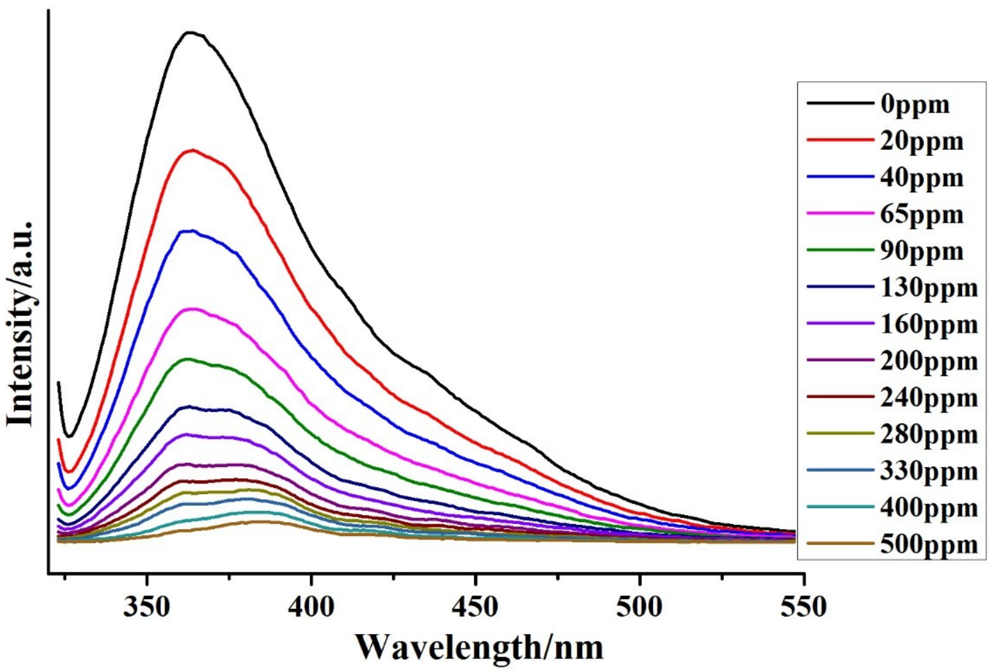

Fig. S16 Luminescent quenching of **1** dispersed in ethanol by the gradual addition of 1 mM solution of 4-NT in DMF.

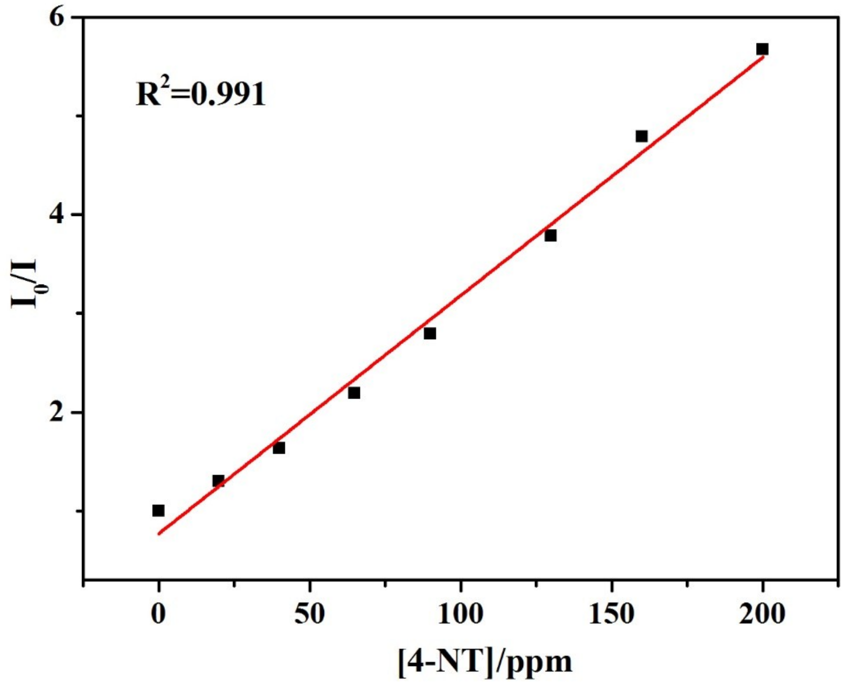

Fig. S17 Stern–Volmer plot for the fluorescence quenching of **1** upon the addition of 4-NT.

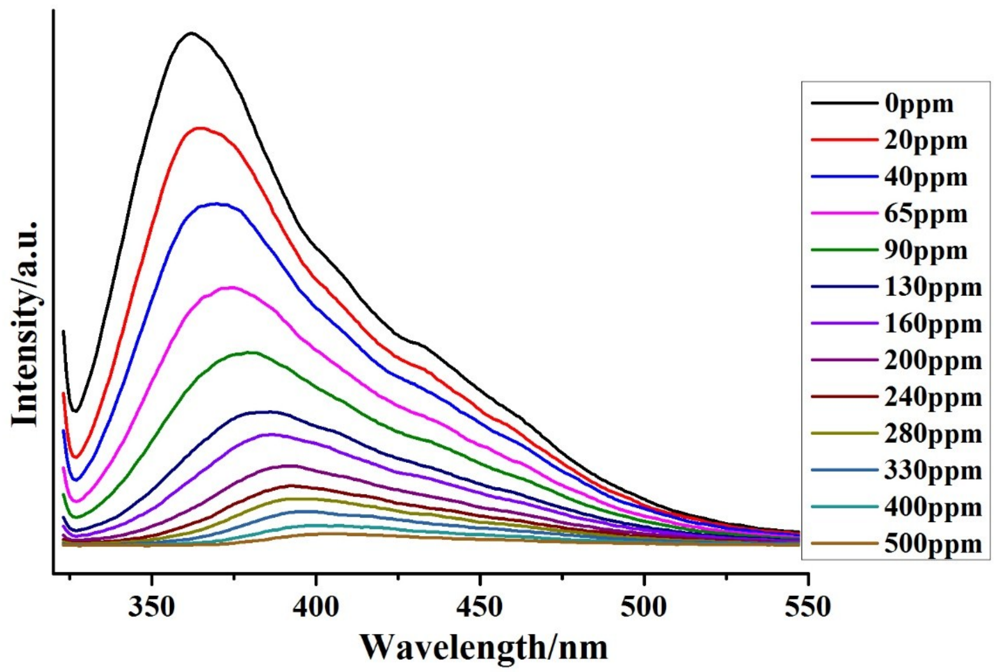

Fig. S18 Luminescent quenching of **1** dispersed in ethanol by the gradual addition of 1 mM solution of MNP in DMF.

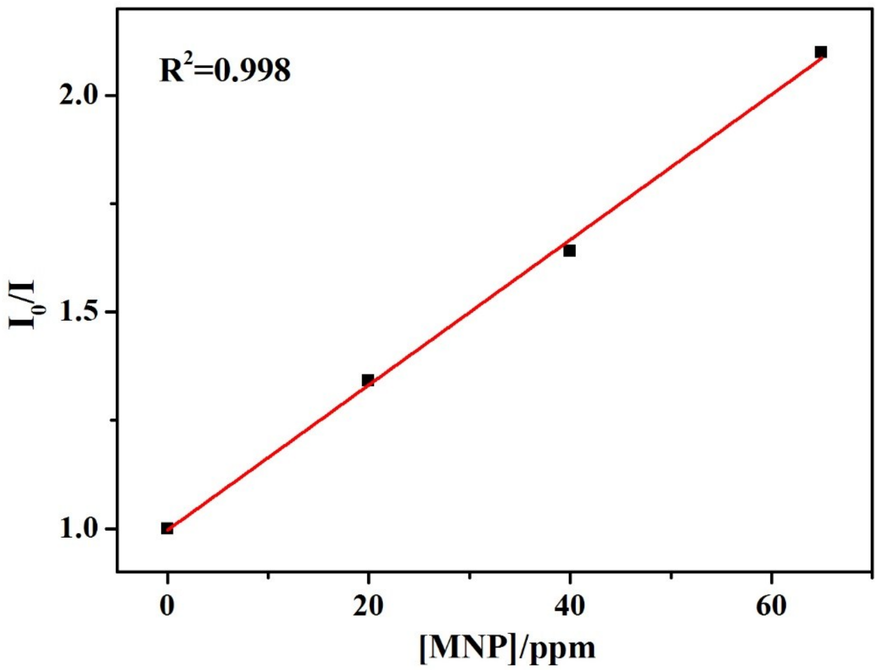

Fig. S19 Stern–Volmer plot for the fluorescence quenching of **1** upon the addition of MNP.

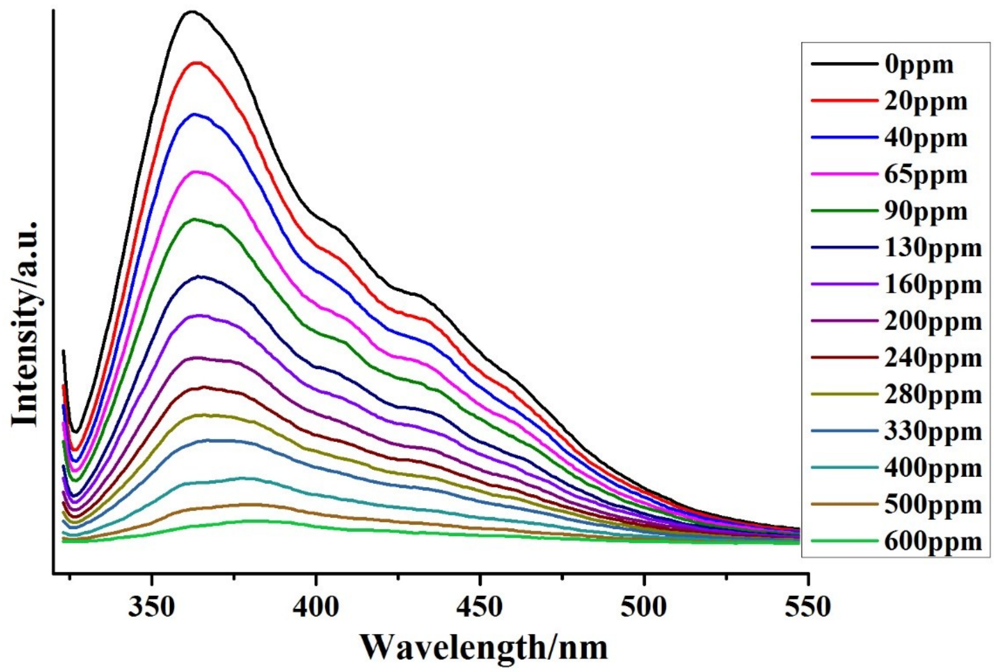

Fig. S20 Luminescent quenching of **1** dispersed in ethanol by the gradual addition of 1 mM solution of NB in DMF.

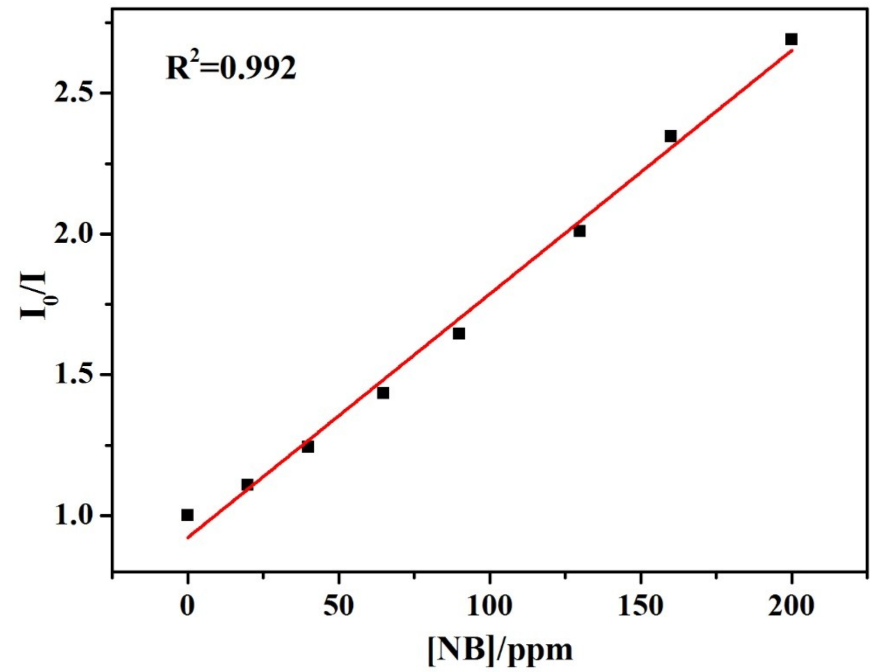

Fig. S21 Stern–Volmer plot for the fluorescence quenching of **1** upon the addition of NB.

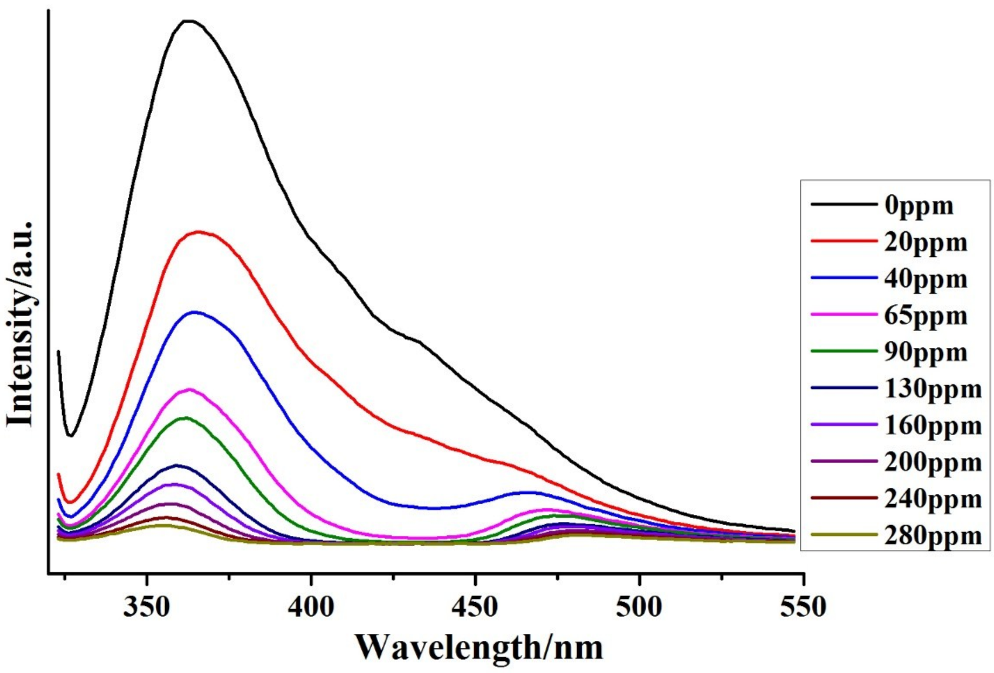

Fig. S22 Luminescent quenching of **1** dispersed in ethanol by the gradual addition of 1 mM solution of PNP in DMF.

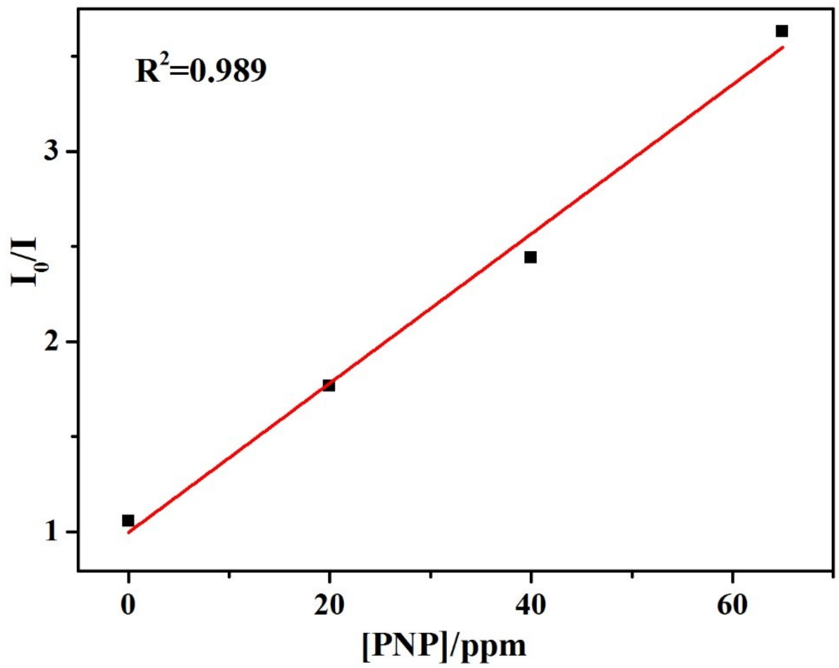

Fig. S23 Stern–Volmer plot for the fluorescence quenching of **1** upon the addition of PNP.

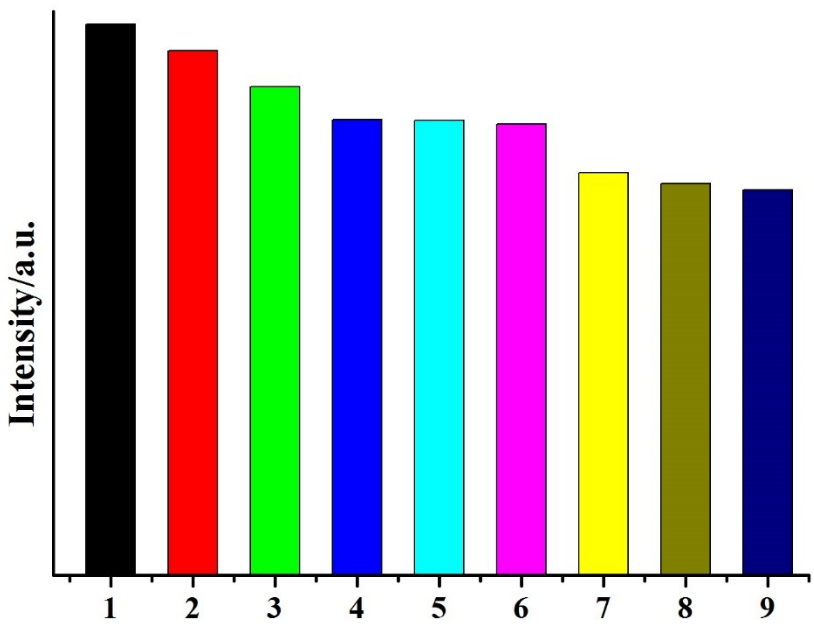

Fig. S24 Luminescent quenching of H_4L dispersed in ethanol by the gradual addition of 1 mM solution of 2,4-DNP in DMF (from 0-240 ppm).

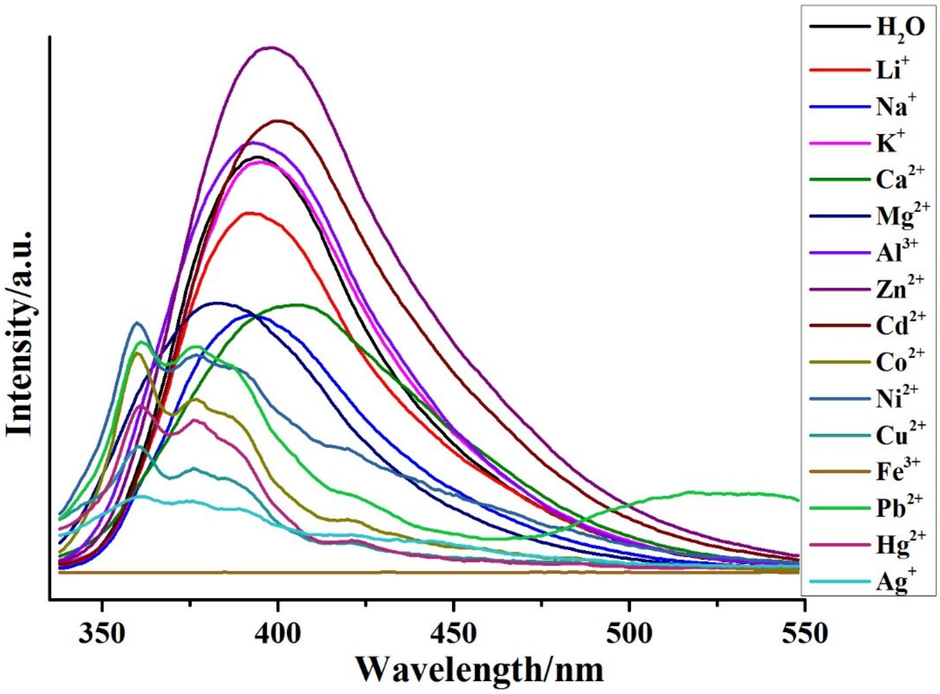

Fig. S25 Emission spectra of **1** at different metal ions.

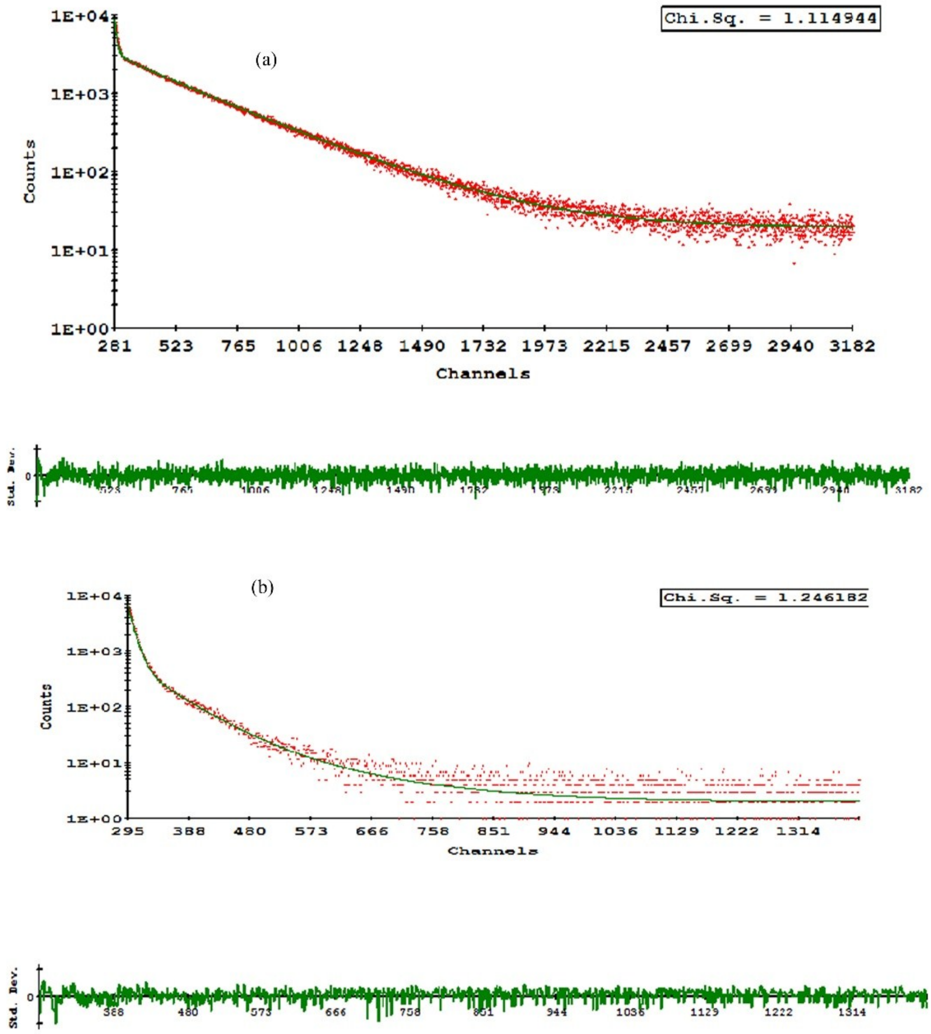

Fig. S26 Comparison of the fluorescence lifetime of **1** (above) and Fe^{3+}@ **1** (below).

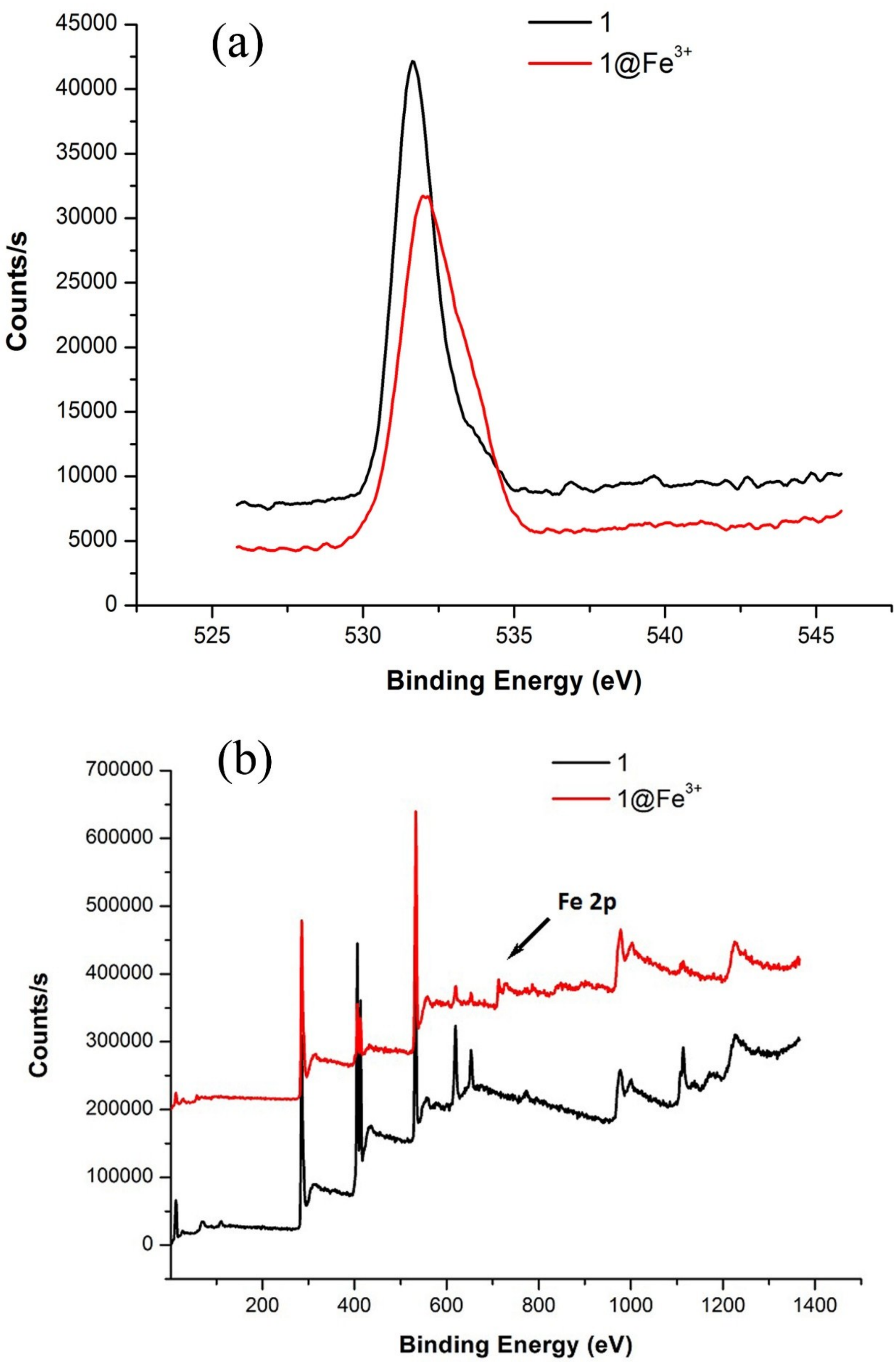

Fig. S27. (a) O1s XPS spectra of the original **1** (black) and **1**@Fe^{3+} (red); (b) XPS spectra of the **1**@Fe^{3+} (red) and original **1** (black).

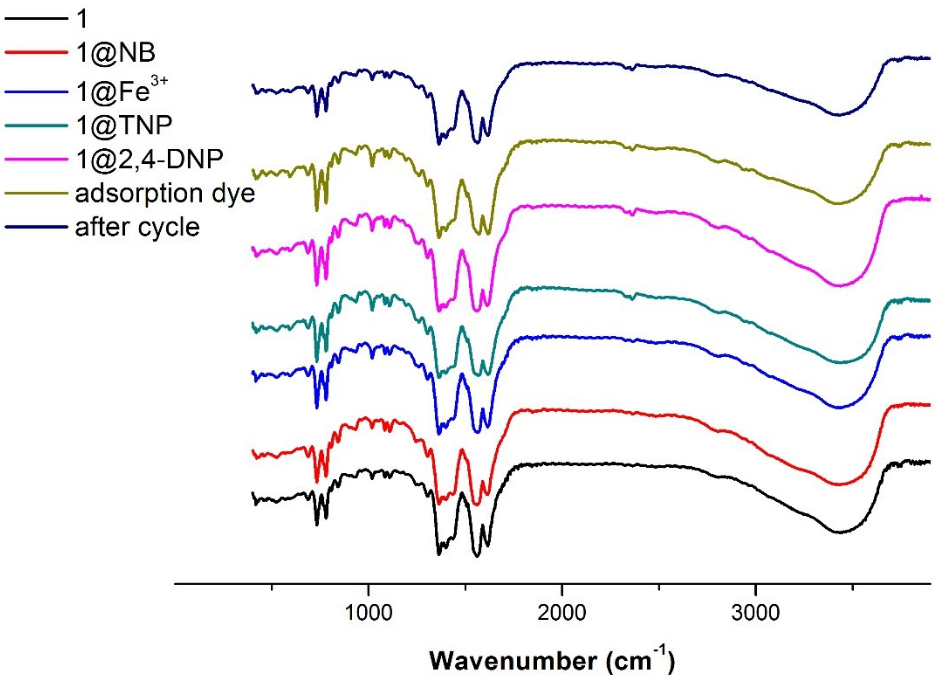

Fig. S28 IR spectra of **1** and **1** in different dispersion samples.

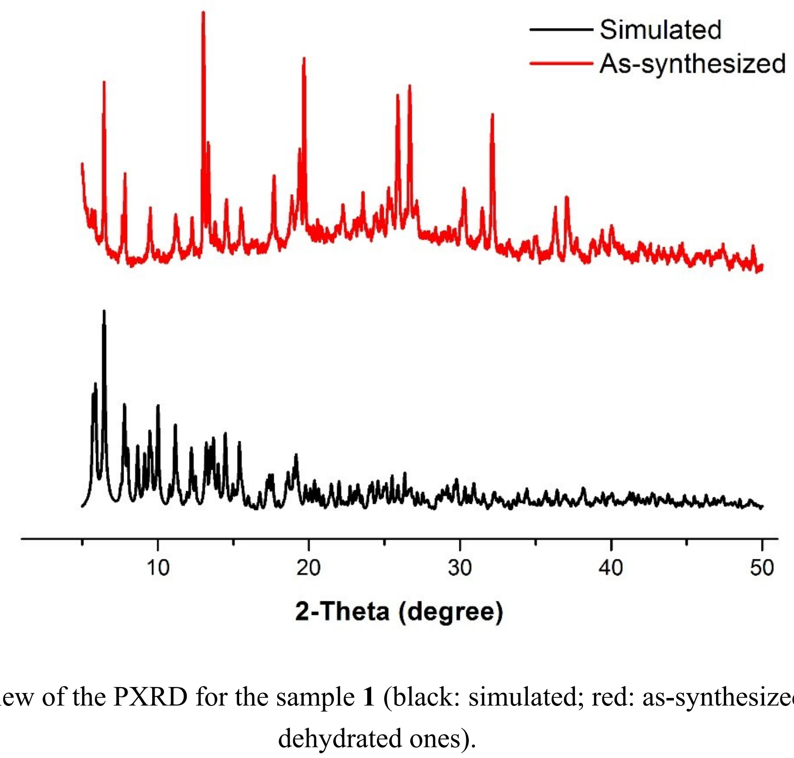

Fig. S29 view of the PXRD for the sample **1** (black: simulated; red: as-synthesized; blue: dehydrated ones).

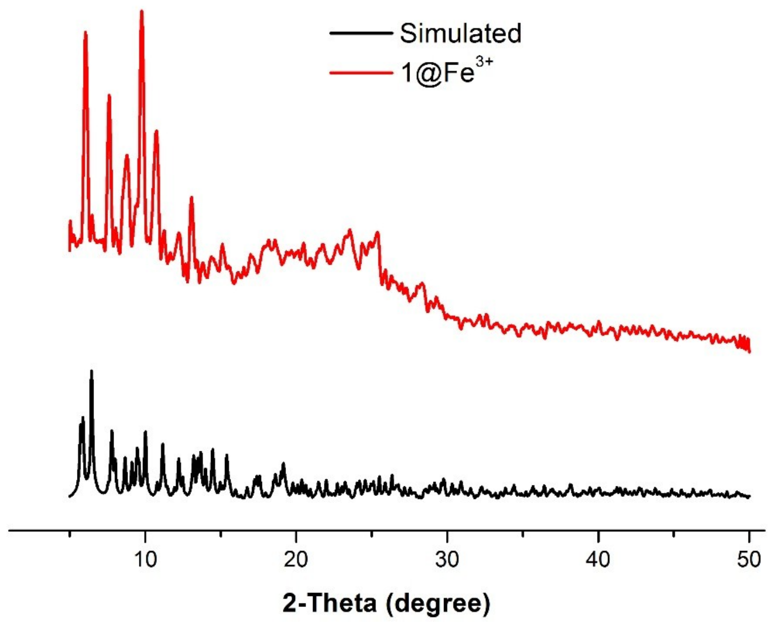

Fig. S30 view of the PXRD pattern of **1**@Fe^{3+} sample.

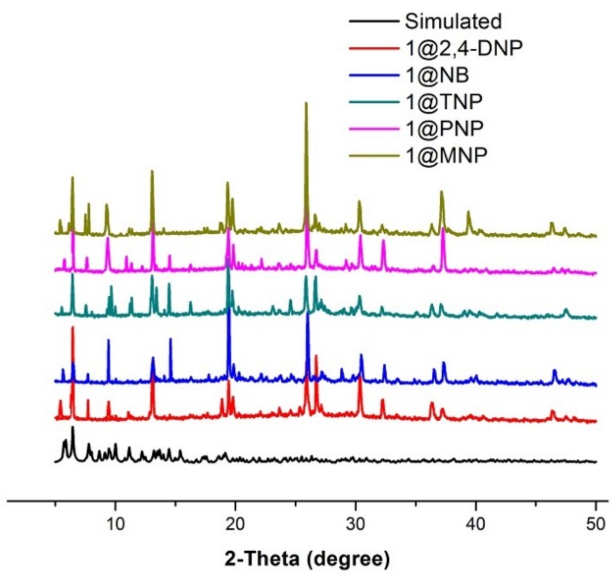

Fig. S31 view of the PXRD pattern of **1** dispersed in different explosives.

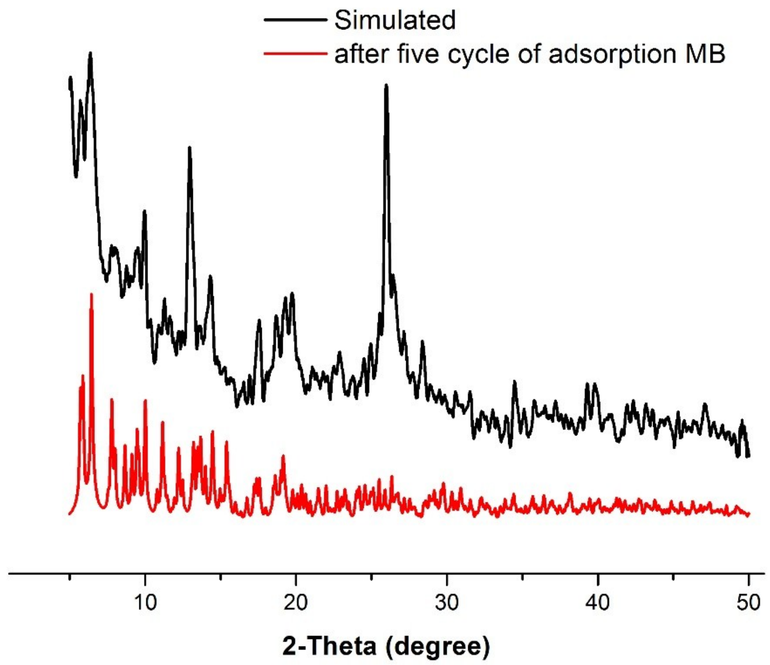

Fig. S32 view of the PXRD pattern of **1** after five cycle of adsorption of MB.

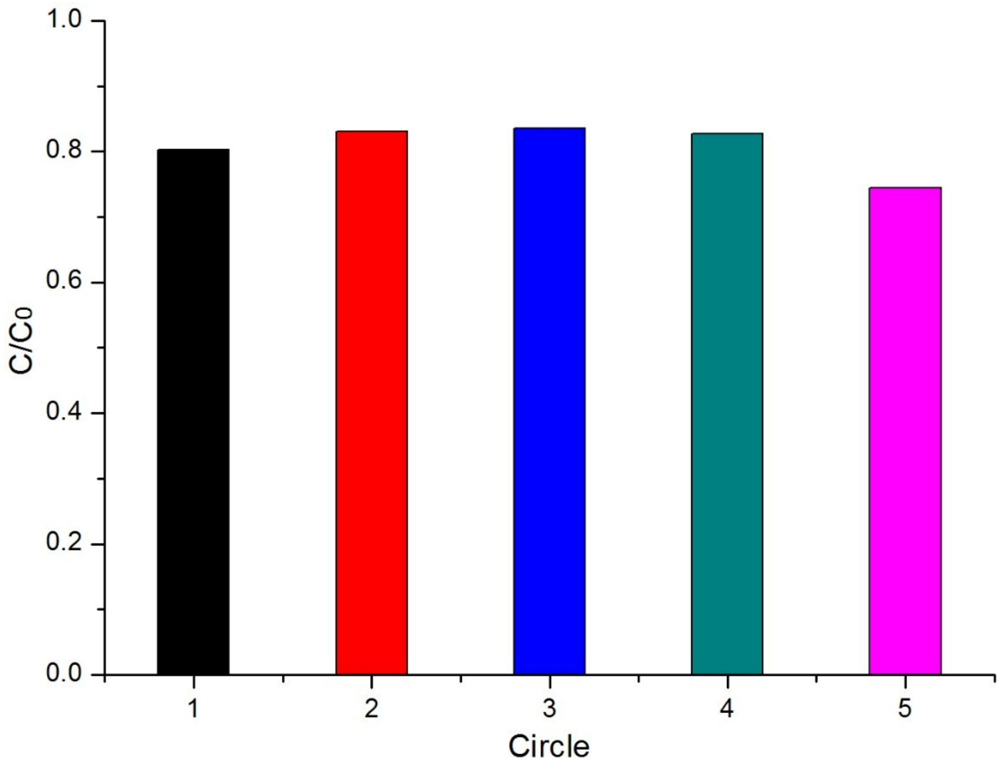

Fig. S33 view the adsorption ability for the MB in **1** after 5 cycle.

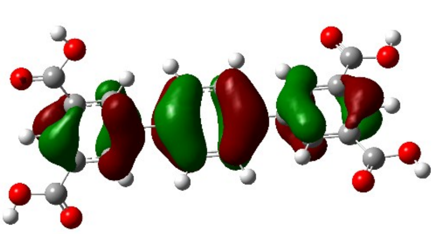 HOMO H_4L	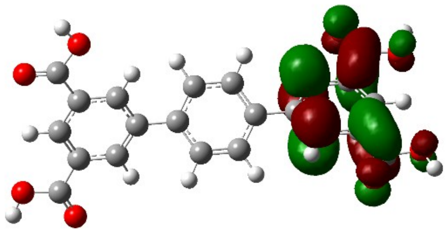 LUMO H_4L
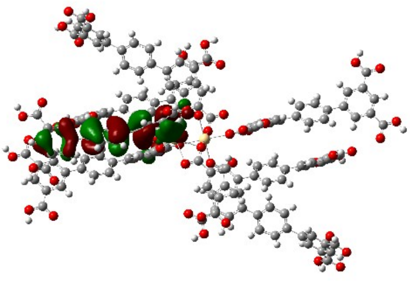 HOMO **1**	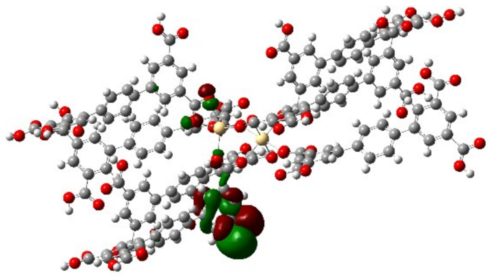 LUMO **1**
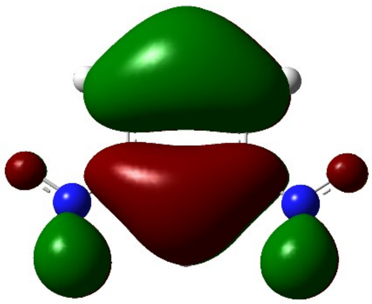 HOMO 1,3-DNB	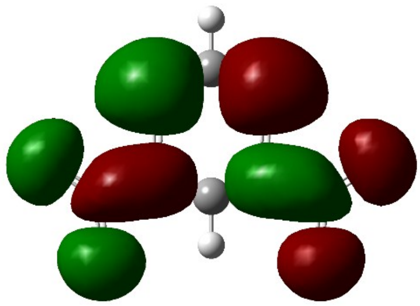 LUMO 1,3-DNB
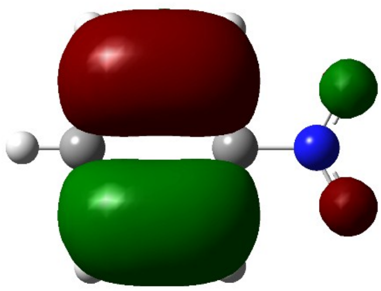 HOMO NB	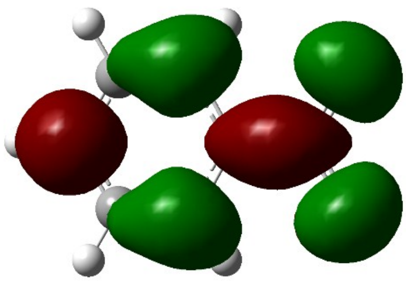 LUMO NB
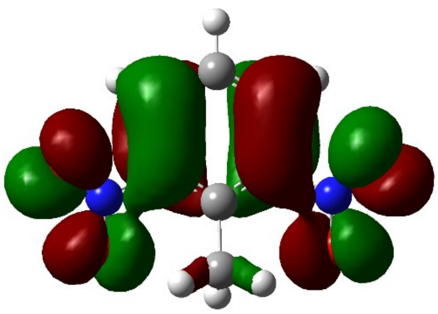 HOMO 2,6-DNT	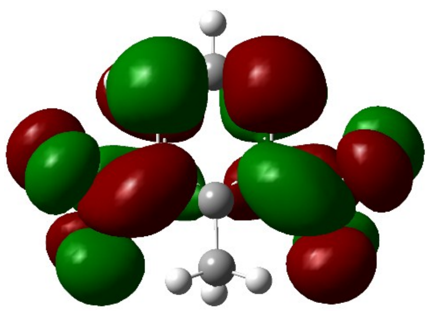 LUMO 2,6-DNT

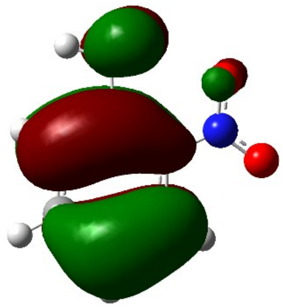 HOMO 2-NT	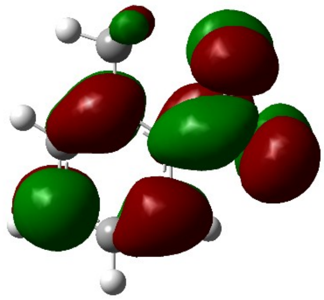 LUMO 2-NT
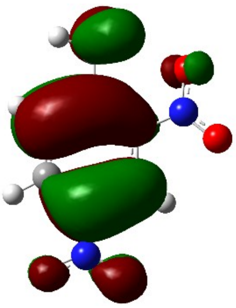 HOMO 2,4-DNT	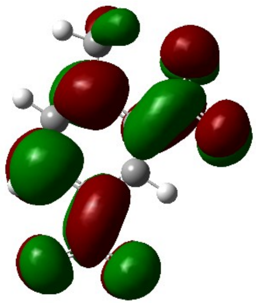 LUMO 2,4-DNT
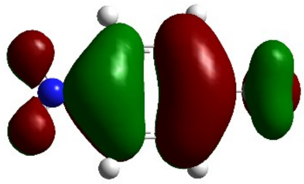 HOMO 4-NT	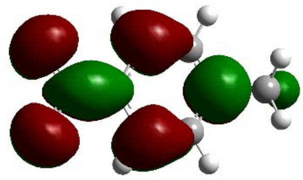 LUMO 4-NT
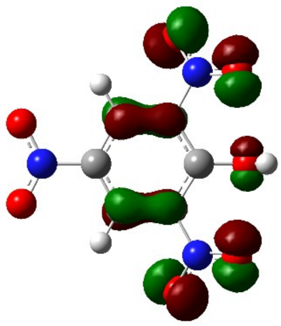 HOMO TNP	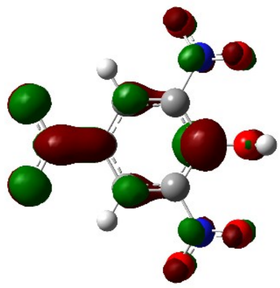 LUMO TNP

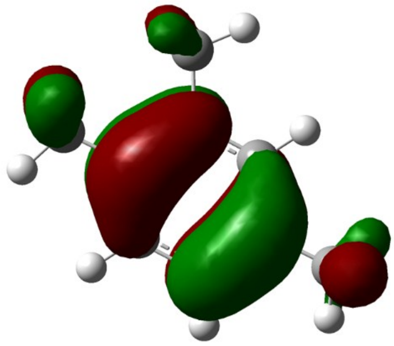 HOMO 1,2,4-TMB	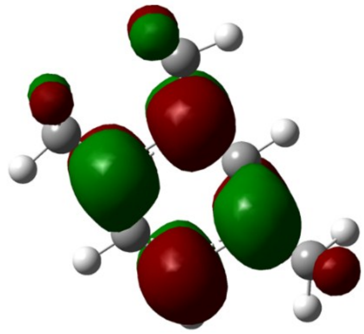 LUMO 1,2,4-TMB
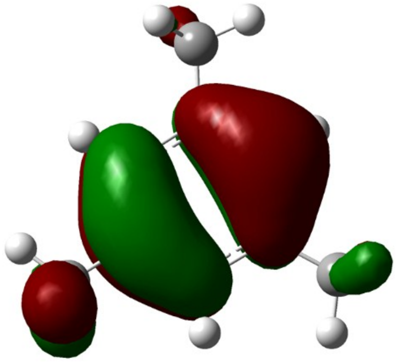 HOMO 1,3,5-TMB	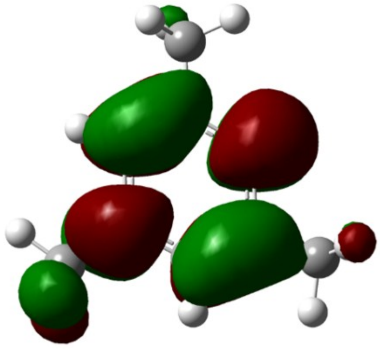 LUMO 1,3,5-TMB
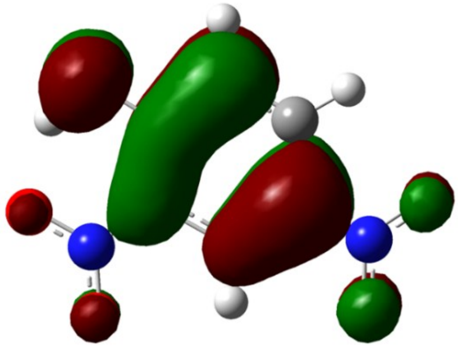 HOMO 2,4-DNP	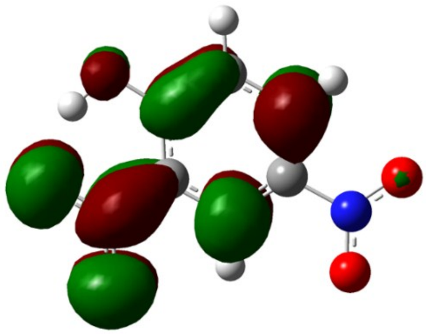 LUMO 2,4-DNP
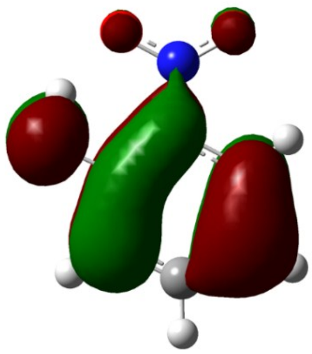 HOMO *o*-nitro phenol	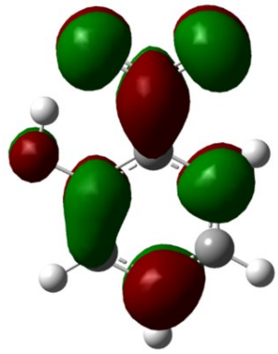 LUMO *o*-nitro phenol

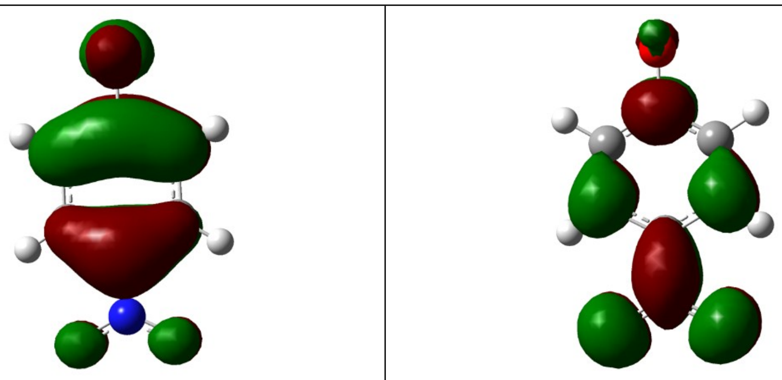

HOMO *p*-nitrophenol | LUMO *p*-nitrophenol

Fig. S34 HOMO–LUMO energies of the NACs along with MOF **1** and H_4L.

Table S1 Crystal data and structure refinement for 1.

Empirical formula	$C_{109}N_9O_{36}Cd_5H_{111}$
Temperature/K	100.15
Crystal system	monoclinic
Space group	$P2_1/c$
a/Å	15.3011(10)
b/Å	18.6188(12)
c/Å	27.6436(18)
α/°	90
β/°	101.2350(10)
γ/°	90
Volume/Å^3	7724.4(9)
Z	2
ρ_{calc}g/cm^3	0.933
μ/mm^{-1}	0.724
F(000)	2128.0
Crystal size/mm^3	0.17 × 0.14 × 0.11
Radiation	MoKα (λ = 0.71073)
2Θ range for data collection/°	3.004 to 55.196
Index ranges	$-19 \leq h \leq 19$, $-24 \leq k \leq 23$, $-36 \leq l \leq 17$
Reflections collected	46064
Independent reflections	17521 [R_{int} = 0.0472, R_{sigma} = 0.0671]
Data/restraints/parameters	17521/24/565
Goodness-of-fit on F^2	1.083
Final R indexes [I>=2σ (I)]	R_1 = 0.0727, wR_2 = 0.2264
Final R indexes [all data]	R_1 = 0.0991, wR_2 = 0.2449
Largest diff. peak/hole / e Å^{-3}	2.17/-0.92

Table S2 Bond Lengths and Angles for 1.

Atom	Atom	Length/Å
Cd01	O16	2.306(4)
Cd01	$O16^1$	2.306(4)
Cd01	O1	2.232(4)
Cd01	$O1^1$	2.232(4)
Cd01	$O10^2$	2.297(4)
Cd01	$O10^3$	2.297(4)
Cd02	$O16^1$	2.365(4)
Cd02	$O15^1$	2.390(5)
Cd02	O2	2.193(5)
Cd02	$O6^4$	2.366(6)
Cd02	$O5^4$	2.320(5)
Cd02	$O9^2$	2.218(6)
Cd03	$O4^5$	2.353(5)
Cd03	$O14^6$	2.358(5)
Cd03	$O3^5$	2.407(5)
Cd03	O8	2.360(5)
Cd03	O7	2.360(6)
Cd03	$O13^6$	2.363(5)

Atom	Atom	Atom	Angle/°
$O16^1$	Cd01	O16	180.0
O1	Cd01	O16	90.58(17)
$O1^1$	Cd01	O16	89.42(17)
O1	Cd01	$O16^1$	89.42(17)
$O1^1$	Cd01	$O16^1$	90.58(17)
O1	Cd01	$O1^1$	180.0
O1	Cd01	$O10^2$	88.53(17)
$O1^1$	Cd01	$O10^3$	88.53(17)
$O1^1$	Cd01	$O10^2$	91.47(17)
O1	Cd01	$O10^3$	91.47(17)
$O10^2$	Cd01	O16	92.44(17)
$O10^2$	Cd01	$O16^1$	87.56(17)
$O10^3$	Cd01	$O16^1$	92.44(17)
$O10^3$	Cd01	O16	87.56(17)

O10[3]	Cd01	O10[2]	180.0(3)
O16[1]	Cd02	O15[1]	55.56(14)
O16[1]	Cd02	O6[4]	96.84(17)
O16[1]	Cd02	C41[1]	28.28(16)
O16[1]	Cd02	C20[4]	121.6(2)
O15[1]	Cd02	C41[1]	27.28(17)
O15[1]	Cd02	C20[4]	93.8(2)
O2	Cd02	O16[1]	100.71(16)
O2	Cd02	O15[1]	156.21(17)
O2	Cd02	O6[4]	94.1(2)
O2	Cd02	O5[4]	104.6(2)
O2	Cd02	O9[3]	93.5(2)
O2	Cd02	C41[1]	128.96(19)
O2	Cd02	C20[4]	101.7(2)
O6[4]	Cd02	O15[1]	90.9(2)
O6[4]	Cd02	C41[1]	94.6(2)
O6[4]	Cd02	C20[4]	28.7(2)
O5[4]	Cd02	O16[1]	143.88(18)
O5[4]	Cd02	O15[1]	97.5(2)
O5[4]	Cd02	O6[4]	56.36(18)
O5[4]	Cd02	C41[1]	121.7(2)
O5[4]	Cd02	C20[4]	27.7(2)
O9[3]	Cd02	O16[1]	109.2(2)
O9[3]	Cd02	O15[1]	93.3(2)
O9[3]	Cd02	O6[4]	150.9(2)
O9[3]	Cd02	O5[4]	94.6(2)
O9[3]	Cd02	C41[1]	102.2(2)
O9[3]	Cd02	C20[4]	122.2(2)
C20[4]	Cd02	C41[1]	109.5(2)
O4[5]	Cd03	O14[6]	87.01(16)
O4[5]	Cd03	O3[5]	54.81(16)
O4[5]	Cd03	O8	126.74(18)
O4[5]	Cd03	O7	94.1(2)
O4[5]	Cd03	O13[6]	141.73(16)
O8	Cd03	C42[6]	112.52(19)

[1]-X,-Y,-Z; [2]-1+X,+Y,+Z; [3]1-X,-Y,-Z; [4]1-X,-1/2+Y,1/2-Z; [5]1+X,+Y,+Z; [6]1-X,1-Y,-Z; [7]1-X,1/2+Y,1/2-Z

Table S3 Comparison of the selected materials in detective sensitivity for Fe^{3+} ions

Material	Sensitivity	Reference
$Eu(acac)_3@Zn(C_{15}H_{12}NO_2)_2$	5×10^{-3} M	1
$Eu(C_{33}H_{24}O_{12})(H_2NMe)(H_2O)$	2×10^{-4} M	2
$Eu(C_{22}H_{14}O_2)_3$	10^{-4} M	3
$[Eu(BTPCA)(H_2O)]\cdot2DMF\cdot3H_2O$	10^{-5} M	4
MIL-53(Al)	0.9×10^{-6} M	5
$\{[LnCd_2(DTPA)_2(H_2O)_4]\cdot4H_2O$	1.5×10^{-5} M	6
carbon nanoparticles (CNPs)	0.32×10^{-6} M	7
Fluorescent Gold Nanoclusters	5.4×10^{-6} M	8
$[Cd_3(dpa)(DMF)_2(H_2O)_3]\cdot DMF$	1.75×10^{-4} M	9
$Zn_3L_3(DMF)_2$	10^{-5} M	10
$[[Eu_2(MFDA)_2(HCOO)_2(H_2O)_6]\cdot H_2O$	1.0×10^{-4} M	11
$[Tb_4(OH)_4(DSOA)_2(H_2O)_8]\cdot(H_2O)_8$	10^{-6} M	12
1	2.3×10^{-5} M	*In this work*

[1] G. G. Hou, Y. Liu, Q. K. Liu, J. P. Ma and Y. B. Dong, *Chem. Commun.*2011, ***47***, 10731-10733.

[2] S. Dang, E. Ma, Z.M. Sun and H. J. Zhang, *J. Mater. Chem.* 2012, ***22***, 16920-16926.

[3] M. Zheng, H. Q. Tan, Z. G. Xie, L. G. Zhang, X. B. Jing and Z. C. Sun, *ACS Appl. Mater. Interfaces,* 2013, ***5***, 1078-1083.

[4] Q. Tang, S. X. Liu, Y. W. Liu, J. Miao, S. J. Li, L. Zhang, Z. Shi and Z. P. Zheng, *Inorg. Chem.*2013, ***52***, 2799-2801.

[5] C. X. Yang, H. B. Ren and X. P. Yan, *Anal. Chem.*2013, ***85***, 7441-7446.

[6] Q. Liu, F. Wan, L. X. Qiu, Y. Q. Sun and Y. P. Chen, *RSC Adv.*, 2014, ***4***, 27013-27021.

[7] K. G. Qu, J. S. Wang, J. S. Ren and X. G. Qu, *Chem. Eur. J.* 2013, ***19***, 7243-7249.

[8] J.-A. A. Ho, H.-C. Chang and W.-T. Su, *Anal. Chem*. 2012, ***84***, 3246-3253.
[9] J. C. Jin, L. Y. Pang, G. P. Yang, L. Hou and Y. Y. Wang, *Dalton Trans*., 2015, ***44***, 17222–17228.
[10] Z. C. Yu, F. Q. Wang, X. Y. Lin, C. M. Wang, Y. Y. Fu, X. J. Wang, Y. N. Zhao and G. D. Li, *J. Solid. State. Chem*., 2015, ***232***, 96-101.
[11] X. H. Zhou, L. Li, H. H. Li, T. Yang and W. Huang, *Dalton Trans*., 2013, **42**, 12403–12409.
[12] X. Y. Dong, R. Wang, J. Z. Wang, S. Q. Zang and T. C. W. Mak, *J. Mater. Chem*. A, 2015, ***3***, 641–647.

Table S4 Comparison of the selected materials in detective sensitivity for TNP.

Material	NACs	K_{sv}	Reference
BUT-12	TNP	3.1×10^5	1
BUT-13	TNP	5.1×10^5	1
$\{[Zn(C_{34}H_{18}O_8)_{0.5}(C_{20}N_2H_{16})_{0.5}].[0.5(C_{20}N_2H_{16}).2H_2O]\}_n$	TNP	8.1×10^4	2
$[Cd(ndc)_{0.5}(pca)]$	TNP	3.5×10^4	3
$\{[Eu_2(mfda)_2(HCOO)_2(H_2O)_6]\cdot H_2O\}_n$	TNP	5.5×10^4	4
$[Eu_3(bpydb)_3(HCOO)(\mu_3\text{-}OH)_2(H_2O)]$	TNP	2.1×10^4	5
[Tb(1,3,5-BTC)]	TNP	3.42×10^4	6
UiO-67-dcppy	TNP	2.9×10^4	7
1	TNP	1.61×10^4	*In this work*

1.B. Wang, X. L. Lv, D. W. Feng, L. H. Xie, J. Zhang, M. Li, Y. Xie, J. R. Li and H. C. Zhou, *J. Am. Chem. Soc*. 2016, **138**, 6204−6216
2. S. Sanda, S. Parshamoni, S. Biswas and Sanjit Konar, *Chem. Commun.,* 2015, **51**, 6576—6579
3. S. S. Nagarkar, B. Joarder, A. K. Chaudhari, S. Mukherjee and S. K. Ghosh, *Angew. Chem., Int. Ed*., 2013, **52**, 2881–2885.
4.X. H. Zhou, L. Li, H. H. Li, A. Li, T. Yang and W. Huang, Dalton Trans., 2013, **42**, 12403–12409.
5. S. S. Nagarkar, A. V. Desai and S. K. Ghosh, *Chem. Commun*., 2014, **50**, 8915–8918.
6. X.-Z. Song, S.-Y. Song, S.-N. Zhao, Z.-M. Hao, M. Zhu, X. Meng, L.-L. Wu and H.-J. Zhang, *Adv. Funct. Mater*., 2014, **24**, 4034–4041.
7. J.-D. Xiao, L.-G. Qiu, F. Ke, Y.-P. Yuan, G.-S. Xu, Y.-M. Wang and X. Jiang, *J. Mater. Chem. A*, 2013, **1**, 8745–8752.

Selective adsorption behavior for dyes

Typically, 30 mg of adsorbent sample was immersed in 20 mL of aqueous dye solution containing 5×10^{-5} mol L^{-1} of dye at room temperature; the adsorption system was continually stirred.

Parameter meaning

Q_{eq} (mg g^{-1}) is the amount of adsorbed MB by **1**, C_0 (mg L^{-1}) is the initial concentration of MB in the water, and C_{eq} (mg L^{-1}) is the final concentration of MB remaining in the water. V (L) is the volume of MB solution and m (g) is the weight of **1** in this adsorption experiment.

where q_e and q_t (mg g^{-1}) are the amounts of dye adsorbed at equilibrium and t (time), respectively, and K_1 (min^{-1}) is the rate constant.

where K_2 (g mg^{-1} min^{-1}) is the pseudo-second-order rate constant.

where K_3 (g mg^{-1} min^{-1}) is the second-order rate constant.

where K_4 (mg g^{-1} $min^{-1/2}$) is the intraparticle diffusion rate constant and C is the boundary layer thickness.